DOI:
10.1016/j.bbi.2018.09.017

Document Version
Peer reviewed version

Myelination induction by a histamine H3 receptor antagonist in a mouse model of preterm white matter injury

Claire-Marie Rangon [a,b,1], Anne-Laure Schang [a,b, c,1], Juliette Van Steenwinckel [a,b], Leslie Schwendimann [a,b], Sophie Lebon [a,b], Tingting Fu [d], Libo Chen [d], Veronique Beneton [e], Nathalie Journiac [a,b], Pierrette Young-Ten [a,b], Thomas Bourgeois [a,b], Johanna Maze [a,b], Boris Matrot [a,b], Ana A Baburamani [f], Veena Supramaniam [f], Carina Mallard [g], Lionel Trottet [e], A David Edwards [f], Henrik Hagberg [f,g,h], Bobbi Fleiss [a,b,f,l *], Jingjun Li [j], Tsu Tshen Chuang [j,2], Pierre Gressens [a,b,f,2]

[a] PROTECT, INSERM, Université Paris Diderot, Sorbonne Paris Cité, F-75019 Paris, France

[b] PremUP, F-75006 Paris, France

[c] UMR CNRS 8638-Chimie Toxicologie Analytique et Cellulaire, Université Paris Descartes, Sorbonne Paris Cité, Faculté de Pharmacie de Paris, 4 Avenue de l'Observatoire, F-75006 Paris, France

[d] Platform Technologies and Science, GlaxoSmithKline R&D, Shanghai 201203, China; Stevenage, SG1 2NY, UK

[e] Flexible Discovery Unit, Les Ulis, France

[f] Centre for the Developing Brain, School of Biomedical Engineering & Imaging Sciences, King's College London, King's Health Partners, St. Thomas' Hospital, London, SE1 7EH, United Kingdom.

[g] Department of Physiology, Institute of Neuroscience and Physiology, Sahlgrenska Academy, University of Gothenburg, Sweden

[h] Department of Clinical Sciences, Sahlgrenska Academy/East Hospital, 416 85 Gothenburg, Sweden.

[i] School of Health and Biomedical Sciences, RMIT University, Bundoora, VIC, Australia

[j] Regenerative Medicine DPU, GlaxoSmithKline, Shanghai 201023, China; Gunnels Wood Road, Stevenage, Hertfordshire SG1 2NY, UK

* Corresponding author Bobbi Fleiss: RMIT University - Bundoora Campus. Plenty Rd., Bundoora, Victoria, Australia, 3083; bobbi.fleiss@rmit.edu.au

[1] Joint first authorship

[2] Joint last authorship

Authorship and Contributorship

JVS, ALS, BF, LS, SL, NJ, PYT, TB, JM, BM, AB, and VS performed the animal experiments, qRT-PCR, and immunohistochemistry. LC and DS performed the formulation work. TF, VB and LT the performed pharmacokinetic analysis. CMR, JVS, ALS, BF, LS, SL, BM, CM, ADE, HH, BF, JI, TTC and PG participated in experimental design, interpretation of data, and preparation of the manuscript.

Words in Abstract- 318
Words in body of Manuscript- 4250
Number of Figures- 10
Number of Tables- 0
Number of Supplementary Figures- 0
Number of Supplementary Tables- 2

Keywords: encephalopathy, prematurity, oligodendrocyte, neuroinflammation, neuroprotection

Abstract

Fifteen million babies are born preterm every year and a significant number suffer from permanent neurological injuries linked to white matter injury (WMI). A chief cause of preterm birth itself and predictor of the severity of WMI is exposure to maternal-fetal infection-inflammation such as chorioamnionitis. There are no neurotherapeutics for this WMI. To affect this healthcare need, the repurposing of drugs with efficacy in other white matter injury models is an attractive strategy. As such, we tested the efficacy of GSK247246, an H3R antagonist/inverse agonist, in a model of inflammation-mediated WMI of the preterm born infant recapitulating the main clinical hallmarks of human brain injury, which are oligodendrocyte maturation arrest, microglial reactivity, and hypomyelination. WMI is induced by mimicking the effects of maternal-fetal infection-inflammation and setting up neuroinflammation. We induce this process at the time in the mouse when brain development is equivalent to the human third trimester; postnatal day (P)1 through to P5 with i.p. interleukin-1β (IL-1β) injections. We initiated GSK247246 treatment (i.p at 7mg/kg or 20mg/kg) after neuroinflammation was well established (on P6) and it was administered twice daily through to P10. Outcomes were assessed at P10 and P30 with gene and protein analysis. A low dose of GSK247246 (7 mg/kg) lead to a recovery in protein expression of markers of myelin (density of Myelin Basic Protein, MBP & Proteolipid Proteins, PLP) and a reduction in macro- and microgliosis (density of ionising adaptor protein, IBA1 & glial fibrillary acid protein, GFAP). Our results confirm the neurotherapeutic efficacy of targeting the H3R for WMI seen in a cuprizone model of multiple sclerosis and a recently reported clinical trial in relapsing-remitting multiple sclerosis patients. Further work is needed to develop a slow release strategy for this agent and test its efficacy in large animal models of preterm infant WMI.

1. Introduction

The central and peripheral immune systems directly influence the cellular and hence functional integrity of the brain. The immune factors involved in an inflammatory response can provoke beneficial as well as deleterious effects, and their imbalance contributes to the aetiology of many neurodegenerative diseases (Hagberg et al., 2015; Yang et al., 2002). One such condition is brain damage in prematurely born infants, a condition of societal concern due to its continuing increase in incidence without available treatments (Lim et al., 2012; Mento and Nosarti, 2015). Every year 15 million babies are born before 37 weeks of gestation, accounting for approximately 11% of all live births globally(WHO, 2012; Blencowe et al., 2012). The frequency and severity of adverse outcomes rise with decreasing gestational age and poorer quality of care, with almost 10% of the infants born before 33 weeks developing cerebral palsy, and approximately 33% developing chronic cognitive and neuropsychiatric disorders (Arnaud et al., 2007; Delobel-Ayoub et al., 2009). However, even when infants are born close to term, they are still at significantly higher risk of lifelong cognitive and psychiatric problems (Heinonen et al., 2015; Mento and Nosarti, 2015).

A significant neuroanatomical feature of the brain damage observed in preterm born infants is a chronic failure in myelination, referred to as preterm white matter injury (PWMI) (Back et al., 2007; Salmaso et al., 2014; Van Steenwinckel et al., 2014; Verney et al., 2012). Myelin is formed by the extensive cellular processes of mature oligodendrocytes, which mature stepwise from oligodendrocyte progenitor cells through the sequential stages of pre-oligodendrocytes and premature oligodendrocytes (for review see, Mitew et al., 2013). Neuropathological analysis of human post-mortem tissues and animal models reveal that the mechanistic substrate of PWMI is multi-fold, including damage due to inflammatory cytokines and oxidative stress (for discourse see, Paneth, 2018). Exposure of the pre-term born infant to inflammation occurs due to maternal-fetal infection-inflammation which is both a cause of pre-term birth(Goldenberg et al., 2008; Malaeb and Dammann, 2009) and a chief predictor of brain injury. Maternal-fetal infection-inflammatory insults in preterm born infants come from sources including ascending infections leading to chorioamnionitis that are often sub-clinical (Wu et al.,

2009) and postnatal sepsis (O'Shea et al., 2013). The link to brain injury from these pre-natal and post-natal inflammatory exposures is that systemic inflammation propagates into the brain via endothelial cytokine receptors leading to neuroinflammation(Serrats et al., 2010). The mechanistic substrate by which neuroinflammation damages brain development includes as mentioned above excess cytokine and reactive oxygen species production, but also the disruption of the numerous developmental functions of microglia, reviewed in (Tay et al., 2017). A failure to mature or delayed maturation of OPCs is linked to damage to the processes of developmental myelinogenesis (Billiards et al., 2008; Buser et al., 2012; Verney et al., 2010) and reviewed recently in (van Tilborg et al., 2016). Fortuitously, oligodendrocyte progenitor cells remain in the brain in the same numbers even due to toxic insults associated with PWMI providing a therapeutic opportunity through the induction of these oligodendrocyte progenitor cells to differentiate and mature into myelin-forming oligodendrocytes. Such a therapeutic approach is being developed for multiple sclerosis to induce the remyelination of sclerotic plaques with demyelinated neuronal processes (Fancy et al., 2011; Franklin and Ffrench-Constant, 2008; Franklin et al., 2012). Clinical trials include anti-Lingo antibodies (Tran et al., 2014) and a positive outcome from a trial of the histamine receptor 3 (H3R) antagonist GSK239512 (Schwartzbach et al., 2017). It is conceivable that the same therapeutic approach could also benefit PWMI. However, significant differences exist between PWMI and multiple sclerosis in their disease aetiology, the oligodendrocyte progenitor cells in infants and adults may have different properties, and the drug target mechanism in PWMI is to induce myelinogenesis for the first time, whereas remyelination is the target mechanism in multiple sclerosis. Therefore, proof of principle studies with drugs hypothesized to induce oligodendrocyte progenitor cell maturation are needed in relevant preclinical PWMI models to justify PWMI clinical trials.

High-value targets in the hunt for therapies for multiple sclerosis in the past decade have been the histamine receptors (HR), (see reviews, Panula and Nuutinen, 2013; Saligrama et al., 2012), and the H3R, in particular. As such, the potential neuroprotective role of H3R seems worthy of investigating in perinatal brain injury given the common role of oligodendrocytes mentioned above. Despite sharing a high affinity for histamine, the four HRs have low sequence homology (e.g. H4R shares approximately 37% identity with the

H3R, but less than 20% with the H2R and H1R). HRs are G-protein–coupled receptors (GPCRs), and although there is some reported cell specificity that remains incompletely understood H3R, and H4R share downstream signalling via the Gαi subunit, acting via protein kinase A (PKA) (Hu and Chen, 2017; Panula and Nuutinen, 2013) Furthermore, additional signalling cascades also activated by H3R, include the mitogen-activated protein kinase, phospholipase A2 and phosphoinositide 3-kinase (PI3K) pathways. H3R acts as an autoreceptor in histaminergic neurons and as a heteroreceptor in non-histaminergic neurons and regulate the release of various other neurotransmitters, including GABA, glutamate, acetylcholine and noradrenaline. An H3R-penetrant antagonist / inverse agonist, named GSK247246 was initially identified in an *in vitro* assay for its ability to induce the differentiation of OPCs into oligodendrocytes. Furthermore, GSK247246 has recently been described to enhance remyelination in vivo following demyelination induced by cuprizone (Chen et al., 2017).

In the present study, we tested the myelin-inducing ability of GSK247246 in a mouse model of PWMI induced by neuroinflammation driven by systemic inflammation (Favrais et al., 2011; Krishnan et al., 2017; Shiow et al., 2017). This paradigm mimics the clinical events of clinically silent perinatal infection/inflammation that are common in preterm born infants with WMI (Wu et al., 2009). GSK247246 was administered after the establishment of the injurious inflammatory stimuli to directly assess its restorative abilities in a clinically relevant treatment paradigm. We observed that GSK247246 was able to reverse the blockade of developmental myelination induced by the neuroinflammatory insult in several brain regions, and also appeared to possess anti- neuroinflammatory activity. Our study is the first demonstration of a systemically administered compound capable of reversing the blockade of myelination in a preclinical model of PWMI.

2. Material and Methods

2.1. Animals and induction of neuroinflammatory driven WMI via IL-1β administration

Experimental protocols were approved by the institutional guidelines of the Institut National de la Santé et de la Recherche Scientifique (Inserm) France and met the guidelines for the United States Public Health Service's Policy on Humane Care and Use of Laboratory Animals (NIH, Bethesda, Maryland, USA). The protocol was approved by the Bichat-Robert Debre ethical committee under the reference 2011-14/676-0053. OF1 strain mice purchased from Charles River (L'Arbresle, France) and born in our animal facility were used in all experiments. Animals were housed under a 12 h light-dark cycle, had access to food and water ad libitum and were weaned into same-sex groups at P21. On P1 pups were sexed and where necessary litters were culled to 9-11 pups. Assessments of injury and outcomes were made only in male animals as females do not display PWMI in response to this paradigm. IL-1β exposure to set up a systemic and then complex central neuroinflammatory response was carried out as previously described (Favrais et al., 2011). Briefly, mice received twice a day (bid) from P1 to P4, and once on P5, a 5 µl intra-peritoneal (i.p.) injection of 10µg/kg/injection recombinant mouse IL-1β in phosphate buffered saline (PBS; R&D Systems, Minneapolis, MN) or PBS alone (Figure 1). For immunohistochemical analysis at P10, animals came from at least five litters per group, and at P30 the animals came from at least ten litters per group. For analysis via qRT-PCR, animals came from at least five litters per group.

2.2. Pharmacokinetic and pharmacodynamic studies of GSK247246

GSK247246 (*N*-aryl-1,3,4-oxadiazole-2-amine) has a MW of 341.4, it crosses the blood brain barrier, its solubility is 1.47 mg/ml (HCl salt form) at pH7.4, its hydrophilicity is cLogP=3.4 and its Pharmaceutical Formulation Intermediates score is 4.1. We dissolved GSK247246 in 50 mM of sodium citrate buffer (pH5) at the concentration of 10 mg/ml. A pilot pharmacokinetic study was conducted to enable dose selection for pharmacology study. Male naïve OF1 mice at P10 received an i.p. injection of GSK247246 at the dose of 20 mg/kg. We collected blood and brain samples at 6-time points from 0.5 to 24 hours post dosing, and the samples were analysed using a method based upon protein precipitation with acetonitrile followed by LC/MS/MS analysis (with the precursor-to-

product ion transition: m/z 342.2 -> m/z 135.8). The derived pharmacokinetic parameters of blood and brain, the unbound compound concentrations in brain (determined with unbound fraction in brain tissue, data not shown here), *in vitro* potency in oligodendrocyte progenitor cell differentiation assay and *in vivo* pharmacokinetics data of GSK247246 in adult mice cuprizone demyelination model (unpublished data) were used to predict the efficacious dose and dosing regimen in neonatal mice via compartmental pharmacokinetic modelling and simulation with Phoenix software [WinNonlinTM (WNL), Version 6.3 (Pharsight Corp.)], targeting same or longer coverage above *in vitro* EC90 in the pharmacodynamic study.

For the GSK247246 pharmacodynamic study, neonatal mice received bid from P6 to P10 an 8 µl i.p. injection of a low or high dose of GSK247246 (7 mg/kg and 20 mg/kg, respectively) as determined by pharmacokinetics dose prediction stated above, or 50 mM sodium citrate buffer (pH5) alone (vehicle). At 2 hours post the last injection on P10, blood and brain samples (one hemisphere of the brain) were collected from each mouse to determine drug concentration in blood and brain samples with the same method described above.

2.3. Immunohistochemistry

At P10, we collected brains for preparation of frozen sections following intracardial perfusion with 4% paraformaldehyde-phosphate buffer solution under isofluorane anaesthesia. Brains were post-fixed for 4 h at room temperature and then following at least three days in 30% sucrose in PBS the brains were embedded in 15% sucrose-7.5% gelatine solution and frozen at -80°C before sectioning at 16 µm. At P30 brains were processed to paraffin sections by immediate immersion for 6-7 days in 4% formaldehyde at room temperature before dehydration, embedding in paraffin and sectioning at 12 µm.

Primary antibodies used were anti-cleaved caspase-3 (1:500, Cell Signaling, Beverly, MA, USA), anti-Ki67 (1:1000, BD Biosciences, San Jose, CA, USA), anti-Glial Fibrillary Acidic Protein (GFAP, 1/500, Glostrup, Denmark), anti-IBA1 (1:2000, Wako Pure Chemical Industries, Osaka, Japan), anti-NG2 (1:200, Chemicon, Temecula, CA, USA),

anti-Adenomatosis Polyposis Coli (APC, 1:2000, Calbiochem, CA, USA), anti-Myelin Basic Protein (MBP, 1:500, Chemicon), anti-proteolipid protein 1 (PLP, 1/400, Abcam, Cambridge, UK), anti-myelin-associated glycoprotein (MAG, 1/100, Santa Cruz Biotechnology, Santa Cruz, CA, USA), and anti-NEUN (1:500, Chemicon). Immunohistochemistry staining was performed as previously described (Favrais et al., 2011; Schang et al., 2014). Nuclei were counterstained with DAPI (Sigma, St-Quentin Fallavier, France). A blinded experimenter performed all analyses. The intensity of MBP, PLP and MAG immunostaining was assessed via densitometric analysis as previously described using the ImageJ software package (http:// rsbweb.nih.gov/ij/) (Favrais et al., 2011). Cell counts for cleaved caspase-3, Ki67, GFAP, IBA1, NG2, NEUN and APC were performed in four sections per animal for each defined brain structure and are expressed as positive cells per square micrometre. In addition, to validate the expression of the target H3 receptor, anti-H3R primary antibodies (1:500, Sigma) were tested on sections from control P5 brains processed as described for P10 brains.

2.4. Neural tissue dissociation and magnetic-activated cell sorting

At P5 and P10, we collected brains for cell dissociation and O4-positive and CD11b-positive cell enrichment using a magnetic coupled antibody extraction technique (MACS), as previously described (Krishnan et al., 2017; Schang et al., 2014) and according to the manufacturer's protocol (Miltenyi Biotec, Bergisch Gladbach, Germany). Pre-oligodendrocytes express the O4 antigen on their cell surface (Back et al., 2001). In brief, we pooled brains (n=3 at P5 and n=2 at P10) and after removing the cerebellum and olfactory bulbs they were dissociated using the Neural Tissue Dissociation Kit containing papain. From the resulting brain homogenate cells were enriched by MACS, using the anti-O4 or anti-CD11b MicroBeads and after elution, we centrifuged the isolated cells for 5 minutes at 600 g and then conserved them at -80^{o}C. The purity of the eluted fraction was verified using qRT-PCR for GFAP, NEUN, OLIG2 and IBA1 as previously described (Krishnan et al., 2017; Schang et al., 2014) and revealed gene expression levels 95% lower than found in the respective primary cultures of astrocytes, neurons or microglia.

2.5. Microarray analysis and quantitative reverse-transcriptase polymerase-chain reaction

Miltenyi Biotec performed microarrays on a total of 24 MACS extracted O4 and CD11b enriched cell samples from P5 or P10 mice exposed to IL-1β or PBS (Krishnan et al., 2017). Also, we collected frontal lobes from P10 mice exposed to IL-1β or PBS for mRNA extraction and subsequent qRT-PCR for genes involved in oligodendrocyte maturation and myelination. Preparation of samples for array analysis and qRT-PCR, primer design, and PCR protocol were similar to that previously described (Chhor et al., 2013; Husson et al., 2005; Krishnan et al., 2017). We have supplied primer sequences in Supplementary Table 1. *Gapdh* (glyceraldehyde-3-phosphate dehydrogenase gene) was chosen to standardise the quantitative experiments based on reference gene suitability testing. We expressed the relative quantities of mRNA as the specific ratio between the gene of interest and *Gapdh*.

2.6. Statistical and microarray analysis

For the analysis of Statistical analysis of all data was performed using GraphPad Prism version 7.0 (GraphPad Software, San Diego, CA). For all results, we verified that data was normally distributed with the D'Agostino and Pearson omnibus normality test. We used a one-way ANOVA followed by a Newman-Keuls post hoc test for Gaussian distributions, and a Kruskal-Wallis test followed by a Dunn's post hoc test for non-Gaussian distributed data. The Agilent feature extraction software was used to process microarray image files. We only included signal intensities above background. Signal intensity values were background subtracted and uploaded following instructions by Miltenyi Biotec GmbH (Stefan Tomiuk) and Perkin Elmer (Matt Hudson) into GeneSifter Analysis Edition v4.0 (http://login.genesifter.net/) for further analysis as previously described (Gustavsson et al., 2007). The pre-processed signal intensity values were median normalised, and the gene expression in neuroinflammatory and PBS controls were compared at P5 and P10 using t-test ($p<0.05$) with Benjamini-Hochberg multiple testing correction.

3. Results

3.1. Pharmacokinetic study

3.1.1. Pilot pharmacokinetics and dose selection

Fast distribution to blood and brain equilibrium of GSK247246 (within 30 minutes), a half-life of 3.7 hours in blood and 4.1 hours in the brain, were observed in naïve neonatal mice post single i.p. dose at 20 mg/kg. The average brain-to-blood ratio ranged 6-8 at various time points (Figure 2A). We obtained compartmental pharmacokinetics parameters including volume, absorption and elimination rate constants through a compartmental modelling approach. Specifically, we simulated the different doses based on the pilot pharmacokinetics data at 20 mg/kg. Assuming a direct pharmacokinetics-pharmacodynamic relationship and the same efficacious exposure as cuprizone model, 20 mg/kg bid and 7 mg/kg bid was predicted to introduce free brain concentration higher than *in vitro* EC90 for 22 hours and 16 hours on each day of treatment in mice (pharmacokinetics modelling and simulation results not shown here). We selected two doses in order to demonstrate dose-response in the pharmacodynamic study.

3.1.2. End-phase pharmacokinetics in the pharmacodynamic study

GSK247246 concentrations in blood and brain at 2 hours post last dose were determined. We observed proportional compound concentrations in the blood and the brain in the two groups (Figure 2B), which indicated a linear pharmacokinetics at these two doses. The data at 20 mg/kg was comparable to the blood and brain data in the pilot study, suggesting a negligible accumulation after repeat dosing, which was aligned with relatively short half-lives of GSK247246 in both blood and brain compartments. We observed a consistent brain-to-blood ratio in all animals with an average of 5.4 ± 1.0.

3.2. H3R expression

Immunohistochemistry performed on control P5 brains confirmed the expression of the H3R on both white matter and grey matter cells (Figure 3A-B-C). Microarray data confirmed the expression of the H3R mRNA in O4-positive cells and CD11B-positive cells at both at P5 (Supplementary Table 2), and P10 (not shown, see(Krishnan et al., 2017)) and that neuroinflammation did not affect this expression.

3.3. Oligodendrocytes and myelination

We observed similar damage to oligodendrocytes and myelin proteins as we have previously reported in our model of PWMI associated with systemically driven neuroinflammation at P10 and P30 (Favrais et al., 2011; Schang et al., 2014).

Specifically, at P10, when comparing PBS injected animals to PWMI animal there is a decreased density of APC-positive mature oligodendrocytes (Figure 4A) and an increased density of NG2-positive immature oligodendrocytes (Figure 4B) due to neuroinflammatory injury**.** Animals subjected to neuroinflammation and treated with a low dose of GSK247246 showed a significant reduction of the injury associated increase in the density of NG2-positive cells (Figure 4B). The high dose of GSK247246 had no significant effect on NG2 or APC cell numbers from neuroinflammatory injury only parameters (Figure 4).

Specifically, at P30 when comparing PBS injected animals to PWMI animals in the sensorimotor cortical white matter and the basal ganglia the expression of MBP was significantly reduced (Figure 5); in the anterior commissure, cingulate white matter, corpus callosum and external capsule PLP expression was significantly reduced (Figure 6); and in corpus callosum and cingulate white matter MAG expression was significantly reduced (Figure 7). The administration of 7 mg/kg/injection GSK247246 between P6 and P10 in our model of PWMI prevented the decrease of MBP expression in sensorimotor cortical white matter only (Figure 5A-B); of PLP in the anterior commissure, cingulate white matter and external capsule (Figure 4); and of MAG in the corpus callosum and cingulate white matter (Figure 5). Increasing the dosage of GSK247246 (20 mg/kg/injection) resulted in less widespread neuroprotective effects on myelin markers (Figures 5-7).

Gene expression analysis by qRT-PCR on P10 frontal lobes showed that PWMI group animals had a decreased expression of *Mbp*, *Mag*, *Myelin oligodendrocyte glycoprotein* (*Mog)*, *Gap junction gamma-2* (*Gjc2 or connexin-46*), *Early growth response 1* (*Egr1*) and *Fos* mRNA when compared to controls (Figure 8). Low and high doses GSK247246 further decreased the expression of *Egr1* mRNA, GSK-7 (but not GSK-20) reduced

expression of *Dusp,* but no other significant effect on mRNAs were observed, when compared to the PWMI group (Figure 8).

3.4. Proliferation, cell death, astrocytes, microglia, and neurons

The induction of PWMI via systemically driven neuroinflammation or treatment with GSK247246 did not affect the density of Ki67-positive cells in the ventricular zone at P10 (data not shown). Induction of PWMI caused at P10 an increased density of cleaved caspase-3-positive cells in corpus callosum but not in sensorimotor cortical white matter, cingulate white matter and external capsule (Figure 9). However, overall cell death in this model is very low (≤1 cell per $u\text{m}^2$). The low dose of GSK247246 in our PWMI model had no significant effect on cleaved caspase-3-positive cell number when compared to injury only, but the high dose of GSK247246 significantly exacerbated cell death in three of the four studied regions (Figure 9). There was no significant effect on the density of GFAP-positive cells in the four studied regions at P10 in respect to the effects of the neuroinflammatory challenge, or GSK247246 treatments (Figure 10). However, in the PWMI group at P30 there was a significant increase in the density of GFAP-positive cells in the cingulate white matter but not in the three other studied regions (Figure 9A-B). The low and the high dose of GSK247246 prevented this delayed and persisting astrogliosis induced by systemically driven neuroinflammatory injury (Figure 9A-B). In the PWMI group there was a significant increase in the density of IBA1-positive cells in the cingulate white matter at P10 (Figure 11A) and the sensorimotor cortical white matter at P30 (Figure 11B) but not in the other studied regions. The low dose of GSK247246 prevented this microgliosis in the PWMI group (Figure 10B-C). Induction of PWMI had no effect on the number of NEUN-positive cells in the P30 sensorimotor cortex as previously reported for this model (Favrais et al., 2011) and this was also not altered by treatment with GSK247246 (data not shown).

4. Discussion

In our model of inflammation-associated white matter injury of the preterm born infant, treatment with a low dose of GSK247246 (7 mg/kg), an H3R antagonist/inverse agonist, lead to an improvement in protein expression of markers of myelin and a reduction in gliosis. Of note, we initiated treatment only after the animals had already experienced five full days of harmful neuroinflammation, known to cause maturation blockade of oligodendrocytes (Favrais et al., 2011; Schang et al., 2014). As prenatal exposure to inflammation (Baumbusch et al., 2016; Chafer-Pericas et al., 2015; Tronnes et al., 2014) and prenatal changes in the brain have been observed in infants who go on to be born preterm (Thomason et al., 2017) this efficacy with a delayed start provides significant clinical relevance to our study. Our results confirm the neurotherapeutic effects of targeting the H3R for white matter injury seen in a cuprizone model of multiple sclerosis (Wang et al., 2014) and a recently reported clinical trial in relapsing-remitting multiple sclerosis patients (Schwartzbach et al., 2017). Our animal model is specifically designed to model inflammation of the type found in many preterm born infants whose mothers had sub-clinical infections (McElrath et al., 2008; Palmsten et al., 2018; Wu et al., 2009), in contrast to severe events of sepsis or fulminant chorioamnionitis and funisitis. We wish to highlight that the predominate reason for this is that previous post-mortem data from our lab and from others of preterm born infant neuropathology shows that oligodendrocyte cell death is not a major contributor to injury, but that microgliosis and hypomyelination are observed (Billiards et al., 2008; Verney et al., 2010; Verney et al., 2012). Our animal model captures these clinical features, of very limited cell death, microgliosis and eventual hypomyelination (Favrais et al., 2011; Schang et al., 2014; Van Steenwinckel et al., 2018). Overall the data in this study on neuropathological findings and neuroinflammatory events associated with neuroinflammation alone was similar to what we have published previously (Favrais et al., 2011; Krishnan et al., 2017; Schang et al., 2014; Shiow et al., 2017; Van Steenwinckel et al., 2018).

Unfortunately, in our neuroinflammation-mediated WMI model, the dose of 20 mg/kg of GSK247246 increased cell death in regions of white matter (but not in the cortex) and failed to provide any therapeutic action; we ascribe this effect to pharmacokinetics overshoot. In this study, an oscillating pharmacokinetics was expected during repeat

dosing, with over 10-fold concentration drop from Cmax to Ctrough. This expectation was based on the pharmacokinetic profile and a relatively short half-life of GSK247246 demonstrated in the single-dose pharmacokinetic analysis. However, in order to maintain enough free GSK247246 in the brain for the desired duration, overall GSK247246 concentrations had to be boosted with higher doses, which may have led to unexpected toxicity associated with Cmax. Observations in this study of toxicity due to dose are in contrast to the aforementioned multiple sclerosis model (cuprizone), in which GSK247246 demonstrated the efficacy of remyelination at 30 mg/kg, bid oral dosing in adult C57BL6/J mice, with no observable side effects (Wang et al., 2014). Additional formulation work to stabilise the release of the compound (slow release) or target the drug specifically to oligodendrocytes would allow us to lower the dose while maintaining therapeutic levels of the compound must be critical next steps in the translation of this drug for the perinatal population. In addition to effects of dosing, to understand the differences between toxicity data from the current neonatal model and the adult multiple sclerosis model we should look to differences in oligodendrocyte progenitor cell biology in the developing and adult central nervous system. These include, but are not limited to, differences in antigen markers, growth factor responsiveness, motility, cell cycle, and increased vulnerability to oxidative stress (Craig et al., 2003; Semple et al., 2013; van Tilborg et al., 2016). As such, we cannot rule out that oligodendrocyte progenitor cell sensitivity and tolerability to GSK247246 might differ during development (the process of myelinogenesis) and adulthood (remyelination following demyelination). The potential toxicity related to high dose in neonates might also indicate different tolerability and sensitivity of oligodendrocyte progenitor cells in different pathological conditions, i.e. a peripheral inflammation induced hypomyelination vs. centrally focussed toxin-induced demyelination.

The neurotherapeutic effects of GSK247246 against PWMI are also supported by positive effects of another H3R antagonist/inverse agonist GSK239512 on lesion remyelination in a small cohort of human relapsing-remitting multiple sclerosis patients (Schwartzbach et al., 2017). Modulation of the neuroinflammatory responses are considered to be the chief therapeutic effects of H3R modulation either by direct effects on innate or adaptive

immune cells (Ferreira et al., 2012; Saligrama et al., 2013; Saligrama et al., 2012; Teuscher et al., 2007) discussed further below, or via effects on pathways innervating immune tissues (Krementsov et al., 2013). Nevertheless, direct effects on oligodendrocytes also cannot be excluded in this study. Specifically, in our animal model of white matter injury of the preterm born infant oligodendrocyte maturation arrest is induced via the neuroinflammatory actions of microglia (Krishnan et al., 2017); mimicking observations made by our group and others regarding injury seen in human preterm born infants (Billiards et al., 2008; Verney et al., 2012). As such, an obvious target to improve outcome in this model is a direct action on oligodendrocytes to stimulate maturation, and as such myelination. Oligodendrocytes express the H3R protein, and H3R mRNA constitutively with no effects of PWMI driven by systemic inflammation. This expression of H3R demonstrates that these cells are direct targets, even in the context of neuroinflammatory injury, an important observation as neuroinflammation itself has been shown to modulate cell pathway expression in oligodendrocytes (Gottle et al., 2010). A plausible mechanism for a direct positive effect of GSK247246 on oligodendrocyte maturation is the Ga1 mediated GPRC signalling via H3R. This GPRC signalling pathway is conversely responsible for negatively regulating oligodendrocyte maturation following GPR17 activation, via actions on cAMP-PKA (Fumagalli et al., 2011; Simon et al., 2016).

Further data on oligodendrocytes was our observation of discrepancies between the expression of the myelin proteins (improved with GSK247246) and myelin genes (no change with GSK247246). Two hypothesis arise to explain this, (1) mechanisms of post-translational mRNA modifications and mRNA stability are responsible for protein expression and (2) that the total cortical sampling for mRNA analysis hid the positive regional effects of the drug. Importantly, we are confident that our measures of improved myelin proteins reflect improvements in brain structure that are the aim of this study.

This study expands our understanding of the model of neuroinflammation linked WMI, demonstrating for the first time that there is a delayed (P30 only) astrocytic gliosis, although this was observed only in the corpus callosum. Delayed (or Tertiary) phase changes in the brain effect long-term brain health (Fleiss and Gressens, 2012), and

GSK247246 prevented this delayed white matter astrogliosis. Astrocytes express histamine receptors, including H3R (Xu et al., 2018), to support that astrocytes may be a direct target of GSK247246 but alternatively, it is likely that this reduction in delayed gliosis is an indirect effect caused by improvements in microglia and oligodendrocytes at the earlier time point. As GFAP expression typically reduces with increasing age in the mouse (see review, Middeldorp and Hol, 2011), further work is needed to ascertain whether this change at P30 may represent an altered developmental profile.

Microglial activation plays a role in the pathological processes of almost all injuries and disorders for the brain (Prinz et al., 2011; Siskova and Tremblay, 2013), including our WMI model (Krishnan et al., 2017), with limited exceptions (Chhor et al., 2017). Microglia express all four HR (Ferreira et al., 2012) including in the developing brain (Krishnan et al., 2017). As part of in-house screening for pro-myelinogenic target molecules, via analysis of MBP expression by oligodendrocyte progenitor cells co-cultured with LPS-activated BV2 microglia, this compound improved myelination by modulating microglial activity. That microglia could be a direct target of GSK247246 is further supported by our observations that microglial express mRNA for H3R and that GSK247246 reduced the increase in the density of IBA1-positive microglia in specific brain regions at different ages in our model of PWMI.

We only began administering GSK247246 after animals had been exposed to 5 days of injurious inflammation and we provided twice daily injections of GSK247246 from P6 through to and including P10; we wish to highlight two issues related to this paradigm. Firstly, this paradigm mimics a plausible clinical dosing regimen as pre-natal maternal-fetal infection/inflammation is often clinically silent, and precipitates spontaneous pre-term birth (Hillier et al., 1993; Wu et al., 2009). As such, infants are born following exposure to inflammatory injury, and changes to the brain have been observed prenatally in fetuses later delivered preterm (Thomason et al., 2017). Secondly, we observed while performing this study alongside other projects and compared to historical data that injecting the pups from P5-P10 with PBS in and of itself exacerbated the injury in the IL-1β alone group, who had IL-1β from P1-P5 and then PBS from P6-P10. Experimental

design encompassing heightened / persisting stress is clinically relevant (Brummelte et al., 2012) and reinforces the utility of this drug as a neurotherapeutic with clinical potential.

In summary, in a clinically relevant model of WMI of the preterm infant, low dose treatment with GSK247246 was able to recover injury to the white matter, and reduce micro- and astroglial reactivity. As this drug functions to recover WMI in the immature brain even with a delay to the administration further testing in large preclinical models of white matter injury are justified.

5. Acknowledgements

The authors' research is funded by the Cerebral Palsy Alliance (Australia), Wellcome Trust (WT094823), Inserm, Université Paris Diderot, Fondation Leducq (DSRR_P34404), Fondation Grace de Monaco, Fondation Roger de Spoelberch, PremUP, and Fondation des Gueules Cassées. The authors acknowledge financial support from the Department of Health via the National Institute for Health Research (NIHR) comprehensive Biomedical Research Centre award to Guy's & St Thomas' NHS Foundation Trust in partnership with King's College London and King's College Hospital NHS Foundation Trust. The supporting bodies played no role in any aspect of study design, analysis, interpretation or decision to publish this data. We would like to acknowledge Ryan Wang, Even Wu, Jasminder Sahi, Dominic Sanderson and Julie Holder for sharing their knowledge and helpful discussion.

6. Potential conflict of interest

GSK provided financial funding for this study in the form of research service contract.

7. References

Arnaud, C., Daubisse-Marliac, L., White-Koning, M., Pierrat, V., Larroque, B., Grandjean, H., Alberge, C., Marret, S., Burguet, A., Ancel, P.Y., Supernant, K., Kaminski, M., 2007. Prevalence and associated factors of minor neuromotor dysfunctions at age 5 years in prematurely born children: the EPIPAGE Study. Arch. Pediatr. Adolesc. Med. 161, 1053-1061.

Back, S.A., Luo, N.L., Borenstein, N.S., Levine, J.M., Volpe, J.J., Kinney, H.C., 2001. Late oligodendrocyte progenitors coincide with the developmental window of vulnerability for human perinatal white matter injury. J. Neurosci. 21, 1302-1312.

Back, S.A., Riddle, A., McClure, M.M., 2007. Maturation-dependent vulnerability of perinatal white matter in premature birth. Stroke 38, 724-730.

Baumbusch, M.A., Buhimschi, C.S., Oliver, E.A., Zhao, G.M., Thung, S., Rood, K., Buhimschi, I.A., 2016. High Mobility Group-Box 1 (HMGB1) levels are increased in amniotic fluid of women with intra-amniotic inflammation-determined preterm birth, and the source may be the damaged fetal membranes. Cytokine 81, 82-87.

Billiards, S.S., Haynes, R.L., Folkerth, R.D., Borenstein, N.S., Trachtenberg, F.L., Rowitch, D.H., Ligon, K.L., Volpe, J.J., Kinney, H.C., 2008. Myelin abnormalities without oligodendrocyte loss in periventricular leukomalacia. Brain Pathol. 18, 153-163.

Blencowe, H., Cousens, S., Oestergaard, M.Z., Chou, D., Moller, A.B., Narwal, R., Adler, A., Vera Garcia, C., Rohde, S., Say, L., Lawn, J.E., 2012. National, regional, and worldwide estimates of preterm birth rates in the year 2010 with time trends since 1990 for selected countries: a systematic analysis and implications. Lancet 379, 2162-2172.

Brummelte, S., Grunau, R.E., Chau, V., Poskitt, K.J., Brant, R., Vinall, J., Gover, A., Synnes, A.R., Miller, S.P., 2012. Procedural pain and brain development in premature newborns. Ann. Neurol. 71, 385-396.

Buser, J.R., Maire, J., Riddle, A., Gong, X., Nguyen, T., Nelson, K., Luo, N.L., Ren, J., Struve, J., Sherman, L.S., Miller, S.P., Chau, V., Hendson, G., Ballabh, P., Grafe, M.R., Back, S.A., 2012. Arrested preoligodendrocyte maturation contributes to myelination failure in premature infants. Ann. Neurol. 71, 93-109.

Chafer-Pericas, C., Stefanovic, V., Sanchez-Illana, A., Escobar, J., Cernada, M., Cubells, E., Nunez-Ramiro, A., Andersson, S., Vento, M., Kuligowski, J., 2015. Novel biomarkers in amniotic fluid for early assessment of intraamniotic infection. Free Radic. Biol. Med. 89, 734-740.

Chen, Y., Zhen, W., Guo, T., Zhao, Y., Liu, A., Rubio, J.P., Krull, D., Richardson, J.C., Lu, H., Wang, R., 2017. Histamine Receptor 3 negatively regulates oligodendrocyte differentiation and remyelination. PloS one 12, e0189380.

Chhor, V., Le Charpentier, T., Lebon, S., Ore, M.V., Celador, I.L., Josserand, J., Degos, V., Jacotot, E., Hagberg, H., Savman, K., Mallard, C., Gressens, P., Fleiss, B., 2013. Characterization of phenotype markers and neuronotoxic potential of polarised primary microglia in vitro. Brain. Behav. Immun. 32, 70-85.

Chhor, V., Moretti, R., Le Charpentier, T., Sigaut, S., Lebon, S., Schwendimann, L., Ore, M.V., Zuiani, C., Milan, V., Josserand, J., Vontell, R., Pansiot, J., Degos, V., Ikonomidou, C., Titomanlio, L., Hagberg, H., Gressens, P., Fleiss, B., 2017. Role of microglia in a mouse model of paediatric traumatic brain injury. Brain. Behav. Immun. 63, 197-209.

Craig, A., Ling Luo, N., Beardsley, D.J., Wingate-Pearse, N., Walker, D.W., Hohimer, A.R., Back, S.A., 2003. Quantitative analysis of perinatal rodent oligodendrocyte lineage progression and its correlation with human. Exp. Neurol. 181, 231-240.

Dean, J.M., Moravec, M.D., Grafe, M., Abend, N., Ren, J., Gong, X., Volpe, J.J., Jensen, F.E., Hohimer, A.R., Back, S.A., 2011. Strain-specific differences in perinatal rodent oligodendrocyte lineage progression and its correlation with human. Dev. Neurosci. 33, 251-260.

Delobel-Ayoub, M., Arnaud, C., White-Koning, M., Casper, C., Pierrat, V., Garel, M., Burguet, A., Roze, J.C., Matis, J., Picaud, J.C., Kaminski, M., Larroque, B., Group, E.S., 2009. Behavioral

problems and cognitive performance at 5 years of age after very preterm birth: the EPIPAGE Study. Pediatrics 123, 1485-1492.
Dobbing, J., Sands, J., 1979. Comparative aspects of the brain growth spurt. Early Hum. Dev. 3, 79-83.
Fancy, S.P., Harrington, E.P., Yuen, T.J., Silbereis, J.C., Zhao, C., Baranzini, S.E., Bruce, C.C., Otero, J.J., Huang, E.J., Nusse, R., Franklin, R.J., Rowitch, D.H., 2011. Axin2 as regulatory and therapeutic target in newborn brain injury and remyelination. Nat. Neurosci. 14, 1009-1016.
Favrais, G., van de Looij, Y., Fleiss, B., Ramanantsoa, N., Bonnin, P., Stoltenburg-Didinger, G., Lacaud, A., Saliba, E., Dammann, O., Gallego, J., Sizonenko, S., Hagberg, H., Lelievre, V., Gressens, P., 2011. Systemic inflammation disrupts the developmental program of white matter. Ann. Neurol. 70, 550-565.
Ferreira, R., Santos, T., Goncalves, J., Baltazar, G., Ferreira, L., Agasse, F., Bernardino, L., 2012. Histamine modulates microglia function. J Neuroinflammation 9, 90.
Fleiss, B., Gressens, P., 2012. Tertiary mechanisms of brain damage: a new hope for treatment of cerebral palsy? The Lancet. Neurology 11, 556-566.
Franklin, R.J., Ffrench-Constant, C., 2008. Remyelination in the CNS: from biology to therapy. Nature reviews. Neuroscience 9, 839-855.
Franklin, R.J., Ffrench-Constant, C., Edgar, J.M., Smith, K.J., 2012. Neuroprotection and repair in multiple sclerosis. Nat Rev Neurol 8, 624-634.
Fumagalli, M., Daniele, S., Lecca, D., Lee, P.R., Parravicini, C., Fields, R.D., Rosa, P., Antonucci, F., Verderio, C., Trincavelli, M.L., Bramanti, P., Martini, C., Abbracchio, M.P., 2011. Phenotypic changes, signaling pathway, and functional correlates of GPR17-expressing neural precursor cells during oligodendrocyte differentiation. J. Biol. Chem. 286, 10593-10604.
Goldenberg, R.L., Culhane, J.F., Iams, J.D., Romero, R., 2008. Epidemiology and causes of preterm birth. Lancet 371, 75-84.
Gottle, P., Kremer, D., Jander, S., Odemis, V., Engele, J., Hartung, H.P., Kury, P., 2010. Activation of CXCR7 receptor promotes oligodendroglial cell maturation. Ann. Neurol. 68, 915-924.
Gustavsson, M., Mallard, C., Vannucci, S.J., Wilson, M.A., Johnston, M.V., Hagberg, H., 2007. Vascular response to hypoxic preconditioning in the immature brain. J. Cereb. Blood Flow Metab. 27, 928-938.
Hagberg, H., Mallard, C., Ferriero, D.M., Vannucci, S.J., Levison, S.W., Vexler, Z.S., Gressens, P., 2015. The role of inflammation in perinatal brain injury. Nat Rev Neurol 11, 192-208.
Heinonen, K., Eriksson, J.G., Lahti, J., Kajantie, E., Pesonen, A.K., Tuovinen, S., Osmond, C., Raikkonen, K., 2015. Late preterm birth and neurocognitive performance in late adulthood: a birth cohort study. Pediatrics 135, e818-825.
Hillier, S.L., Witkin, S.S., Krohn, M.A., Watts, D.H., Kiviat, N.B., Eschenbach, D.A., 1993. The relationship of amniotic fluid cytokines and preterm delivery, amniotic fluid infection, histologic chorioamnionitis, and chorioamnion infection. Obstet. Gynecol. 81, 941-948.
Hu, W., Chen, Z., 2017. The roles of histamine and its receptor ligands in central nervous system disorders: An update. Pharmacol. Ther.
Husson, I., Rangon, C.M., Lelievre, V., Bemelmans, A.P., Sachs, P., Mallet, J., Kosofsky, B.E., Gressens, P., 2005. BDNF-induced white matter neuroprotection and stage-dependent neuronal survival following a neonatal excitotoxic challenge. Cereb. Cortex 15, 250-261.
Krementsov, D.N., Wall, E.H., Martin, R.A., Subramanian, M., Noubade, R., Del Rio, R., Mawe, G.M., Bond, J.P., Poynter, M.E., Blankenhorn, E.P., Teuscher, C., 2013. Histamine H(3) receptor integrates peripheral inflammatory signals in the neurogenic control of immune responses and autoimmune disease susceptibility. PloS one 8, e62743.
Krishnan, M.L., Van Steenwinckel, J., Schang, A.L., Yan, J., Arnadottir, J., Le Charpentier, T., Csaba, Z., Dournaud, P., Cipriani, S., Auvynet, C., Titomanlio, L., Pansiot, J., Ball, G., Boardman, J.P., Walley, A.J., Saxena, A., Mirza, G., Fleiss, B., Edwards, A.D., Petretto, E., Gressens, P.,

2017. Integrative genomics of microglia implicates DLG4 (PSD95) in the white matter development of preterm infants. Nat Commun 8, 428.
Lim, S.S., Vos, T., Flaxman, A.D., Danaei, G., Shibuya, K., Adair-Rohani, H., Amann, M., Anderson, H.R., Andrews, K.G., Aryee, M., Atkinson, C., Bacchus, L.J., Bahalim, A.N., Balakrishnan, K., Balmes, J., Barker-Collo, S., Baxter, A., Bell, M.L., Blore, J.D., Blyth, F., Bonner, C., Borges, G., Bourne, R., Boussinesq, M., Brauer, M., Brooks, P., Bruce, N.G., Brunekreef, B., Bryan-Hancock, C., Bucello, C., Buchbinder, R., Bull, F., Burnett, R.T., Byers, T.E., Calabria, B., Carapetis, J., Carnahan, E., Chafe, Z., Charlson, F., Chen, H., Chen, J.S., Cheng, A.T., Child, J.C., Cohen, A., Colson, K.E., Cowie, B.C., Darby, S., Darling, S., Davis, A., Degenhardt, L., Dentener, F., Des Jarlais, D.C., Devries, K., Dherani, M., Ding, E.L., Dorsey, E.R., Driscoll, T., Edmond, K., Ali, S.E., Engell, R.E., Erwin, P.J., Fahimi, S., Falder, G., Farzadfar, F., Ferrari, A., Finucane, M.M., Flaxman, S., Fowkes, F.G., Freedman, G., Freeman, M.K., Gakidou, E., Ghosh, S., Giovannucci, E., Gmel, G., Graham, K., Grainger, R., Grant, B., Gunnell, D., Gutierrez, H.R., Hall, W., Hoek, H.W., Hogan, A., Hosgood, H.D., 3rd, Hoy, D., Hu, H., Hubbell, B.J., Hutchings, S.J., Ibeanusi, S.E., Jacklyn, G.L., Jasrasaria, R., Jonas, J.B., Kan, H., Kanis, J.A., Kassebaum, N., Kawakami, N., Khang, Y.H., Khatibzadeh, S., Khoo, J.P., Kok, C., Laden, F., Lalloo, R., Lan, Q., Lathlean, T., Leasher, J.L., Leigh, J., Li, Y., Lin, J.K., Lipshultz, S.E., London, S., Lozano, R., Lu, Y., Mak, J., Malekzadeh, R., Mallinger, L., Marcenes, W., March, L., Marks, R., Martin, R., McGale, P., McGrath, J., Mehta, S., Mensah, G.A., Merriman, T.R., Micha, R., Michaud, C., Mishra, V., Mohd Hanafiah, K., Mokdad, A.A., Morawska, L., Mozaffarian, D., Murphy, T., Naghavi, M., Neal, B., Nelson, P.K., Nolla, J.M., Norman, R., Olives, C., Omer, S.B., Orchard, J., Osborne, R., Ostro, B., Page, A., Pandey, K.D., Parry, C.D., Passmore, E., Patra, J., Pearce, N., Pelizzari, P.M., Petzold, M., Phillips, M.R., Pope, D., Pope, C.A., 3rd, Powles, J., Rao, M., Razavi, H., Rehfuess, E.A., Rehm, J.T., Ritz, B., Rivara, F.P., Roberts, T., Robinson, C., Rodriguez-Portales, J.A., Romieu, I., Room, R., Rosenfeld, L.C., Roy, A., Rushton, L., Salomon, J.A., Sampson, U., Sanchez-Riera, L., Sanman, E., Sapkota, A., Seedat, S., Shi, P., Shield, K., Shivakoti, R., Singh, G.M., Sleet, D.A., Smith, E., Smith, K.R., Stapelberg, N.J., Steenland, K., Stockl, H., Stovner, L.J., Straif, K., Straney, L., Thurston, G.D., Tran, J.H., Van Dingenen, R., van Donkelaar, A., Veerman, J.L., Vijayakumar, L., Weintraub, R., Weissman, M.M., White, R.A., Whiteford, H., Wiersma, S.T., Wilkinson, J.D., Williams, H.C., Williams, W., Wilson, N., Woolf, A.D., Yip, P., Zielinski, J.M., Lopez, A.D., Murray, C.J., Ezzati, M., AlMazroa, M.A., Memish, Z.A., 2012. A comparative risk assessment of burden of disease and injury attributable to 67 risk factors and risk factor clusters in 21 regions, 1990-2010: a systematic analysis for the Global Burden of Disease Study 2010. Lancet 380, 2224-2260.
Malaeb, S., Dammann, O., 2009. Fetal inflammatory response and brain injury in the preterm newborn. J. Child Neurol. 24, 1119-1126.
McElrath, T.F., Hecht, J.L., Dammann, O., Boggess, K., Onderdonk, A., Markenson, G., Harper, M., Delpapa, E., Allred, E.N., Leviton, A., Investigators, E.S., 2008. Pregnancy Disorders That Lead to Delivery Before the 28th Week of Gestation: An Epidemiologic Approach to Classification. Am. J. Epidemiol. 168, 980-989.
Mento, G., Nosarti, C., 2015. The case of late preterm birth: sliding forwards the critical window for cognitive outcome risk. Transl Pediatr 4, 214-218.
Middeldorp, J., Hol, E.M., 2011. GFAP in health and disease. Prog. Neurobiol. 93, 421-443.
Mitew, S., Hay, C.M., Peckham, H., Xiao, J., Koenning, M., Emery, B., 2013. Mechanisms regulating the development of oligodendrocytes and central nervous system myelin. Neuroscience.
O'Shea, T.M., Shah, B., Allred, E.N., Fichorova, R.N., Kuban, K.C., Dammann, O., Leviton, A., Investigators, E.S., 2013. Inflammation-initiating illnesses, inflammation-related proteins, and cognitive impairment in extremely preterm infants. Brain. Behav. Immun. 29, 104-112.
Organisation, W.H., 2012. Born too soon: the global action report on preterm birth.

Palmsten, K., Nelson, K.K., Laurent, L.C., Park, S., Chambers, C.D., Parast, M.M., 2018. Subclinical and clinical chorioamnionitis, fetal vasculitis, and risk for preterm birth: A cohort study. Placenta 67, 54-60.
Paneth, N., 2018. Hypoxia-ischemia and brain injury in infants born preterm. Dev. Med. Child Neurol. 60, 115.
Panula, P., Nuutinen, S., 2013. The histaminergic network in the brain: basic organization and role in disease. Nature reviews. Neuroscience 14, 472-487.
Prinz, M., Priller, J., Sisodia, S.S., Ransohoff, R.M., 2011. Heterogeneity of CNS myeloid cells and their roles in neurodegeneration. Nat. Neurosci. 14, 1227-1235.
Saligrama, N., Case, L.K., del Rio, R., Noubade, R., Teuscher, C., 2013. Systemic lack of canonical histamine receptor signaling results in increased resistance to autoimmune encephalomyelitis. J. Immunol. 191, 614-622.
Saligrama, N., Noubade, R., Case, L.K., del Rio, R., Teuscher, C., 2012. Combinatorial roles for histamine H1-H2 and H3-H4 receptors in autoimmune inflammatory disease of the central nervous system. Eur. J. Immunol. 42, 1536-1546.
Salmaso, N., Jablonska, B., Scafidi, J., Vaccarino, F.M., Gallo, V., 2014. Neurobiology of premature brain injury. Nat. Neurosci. 17, 341-346.
Schang, A.L., Van Steenwinckel, J., Chevenne, D., Alkmark, M., Hagberg, H., Gressens, P., Fleiss, B., 2014. Failure of thyroid hormone treatment to prevent inflammation-induced white matter injury in the immature brain. Brain. Behav. Immun. 37, 95-102.
Schwartzbach, C.J., Grove, R.A., Brown, R., Tompson, D., Then Bergh, F., Arnold, D.L., 2017. Lesion remyelinating activity of GSK239512 versus placebo in patients with relapsing-remitting multiple sclerosis: a randomised, single-blind, phase II study. J. Neurol. 264, 304-315.
Semple, B.D., Blomgren, K., Gimlin, K., Ferriero, D.M., Noble-Haeusslein, L.J., 2013. Brain development in rodents and humans: Identifying benchmarks of maturation and vulnerability to injury across species. Prog. Neurobiol. 106-107, 1-16.
Serrats, J., Schiltz, J.C., Garcia-Bueno, B., van Rooijen, N., Reyes, T.M., Sawchenko, P.E., 2010. Dual roles for perivascular macrophages in immune-to-brain signaling. Neuron 65, 94-106.
Shiow, L.R., Favrais, G., Schirmer, L., Schang, A.L., Cipriani, S., Andres, C., Wright, J.N., Nobuta, H., Fleiss, B., Gressens, P., Rowitch, D.H., 2017. Reactive astrocyte COX2-PGE2 production inhibits oligodendrocyte maturation in neonatal white matter injury. Glia 65, 2024-2037.
Simon, K., Hennen, S., Merten, N., Blattermann, S., Gillard, M., Kostenis, E., Gomeza, J., 2016. The Orphan G Protein-coupled Receptor GPR17 Negatively Regulates Oligodendrocyte Differentiation via Galphai/o and Its Downstream Effector Molecules. J. Biol. Chem. 291, 705-718.
Siskova, Z., Tremblay, M.E., 2013. Microglia and synapse: interactions in health and neurodegeneration. Neural Plast 2013, 425845.
Tay, T.L., Savage, J.C., Hui, C.W., Bisht, K., Tremblay, M.E., 2017. Microglia across the lifespan: from origin to function in brain development, plasticity and cognition. J Physiol 595, 1929-1945.
Teuscher, C., Subramanian, M., Noubade, R., Gao, J.F., Offner, H., Zachary, J.F., Blankenhorn, E.P., 2007. Central histamine H3 receptor signaling negatively regulates susceptibility to autoimmune inflammatory disease of the CNS. Proc. Natl. Acad. Sci. U. S. A. 104, 10146-10151.
Thomason, M.E., Scheinost, D., Manning, J.H., Grove, L.E., Hect, J., Marshall, N., Hernandez-Andrade, E., Berman, S., Pappas, A., Yeo, L., Hassan, S.S., Constable, R.T., Ment, L.R., Romero, R., 2017. Weak functional connectivity in the human fetal brain prior to preterm birth. Sci Rep 7, 39286.
Tran, J.Q., Rana, J., Barkhof, F., Melamed, I., Gevorkyan, H., Wattjes, M.P., de Jong, R., Brosofsky, K., Ray, S., Xu, L., Zhao, J., Parr, E., Cadavid, D., 2014. Randomized phase I trials of the safety/tolerability of anti-LINGO-1 monoclonal antibody BIIB033. Neurol Neuroimmunol Neuroinflamm 1, e18.

Tronnes, H., Wilcox, A.J., Lie, R.T., Markestad, T., Moster, D., 2014. Risk of cerebral palsy in relation to pregnancy disorders and preterm birth: a national cohort study. Dev. Med. Child Neurol. 56, 779-785.
Van Steenwinckel, J., Schang, A.L., Krishnan, M.L., Degos, V., Delahaye-Duriez, A., Bokobza, C., Verdonk, F., Montame, A., Sigaut, S., Hennebert, O., Lebon, S., Schwendiman, L., Le Charpentier, T., Hassan-Abdi, R., Ball, G., Aljabar, P., Saxena, A., Holloway, R., Birchmeier, W., Auvynet, C., Miron, V., Rowitch, D.H., Chretien, F., Petretto, E.G., Edwards, A.D., Hagberg, H., Soussi-Yanicostas, N., Fleiss, B., Gressens, P., 2018. Loss of the Wnt/β-catenin pathway in microglia of the developing brain drives pro-inflammatory activation leading to white matter injury. Biorxiv preprint.
Van Steenwinckel, J., Schang, A.L., Sigaut, S., Chhor, V., Degos, V., Hagberg, H., Baud, O., Fleiss, B., Gressens, P., 2014. Brain damage of the preterm infant: new insights into the role of inflammation. Biochem. Soc. Trans. 42, 557-563.
van Tilborg, E., Heijnen, C.J., Benders, M.J., van Bel, F., Fleiss, B., Gressens, P., Nijboer, C.H., 2016. Impaired oligodendrocyte maturation in preterm infants: Potential therapeutic targets. Prog. Neurobiol. 136, 28-49.
Verney, C., Monier, A., Fallet-Bianco, C., Gressens, P., 2010. Early microglial colonization of the human forebrain and possible involvement in periventricular white-matter injury of preterm infants. J. Anat. 217, 436-448.
Verney, C., Pogledic, I., Biran, V., Adle-Biassette, H., Fallet-Bianco, C., Gressens, P., 2012. Microglial reaction in axonal crossroads is a hallmark of noncystic periventricular white matter injury in very preterm infants. J. Neuropathol. Exp. Neurol. 71, 251-264.
Wang, R., Chen, Y., Guo, T., Zhen, W., Zhao, R., Liu, A.A., Rubio, J.P., Krull, D., Lu, J., Song, M., Thompson, P., 2014. Histamine H3 receptor negatively regulates oligodendrocyte differentiation and myelination. Mult. Scler. 20(S1).
Wu, H.C., Shen, C.M., Wu, Y.Y., Yuh, Y.S., Kua, K.E., 2009. Subclinical histologic chorioamnionitis and related clinical and laboratory parameters in preterm deliveries. Pediatr Neonatol 50, 217-221.
Xu, J., Zhang, X., Qian, Q., Wang, Y., Dong, H., Li, N., Qian, Y., Jin, W., 2018. Histamine upregulates the expression of histamine receptors and increases the neuroprotective effect of astrocytes. J Neuroinflammation 15, 41.
Yang, M.S., Park, E.J., Sohn, S., Kwon, H.J., Shin, W.H., Pyo, H.K., Jin, B., Choi, K.S., Jou, I., Joe, E.H., 2002. Interleukin-13 and -4 induce death of activated microglia. Glia 38, 273-280.

8. Figures

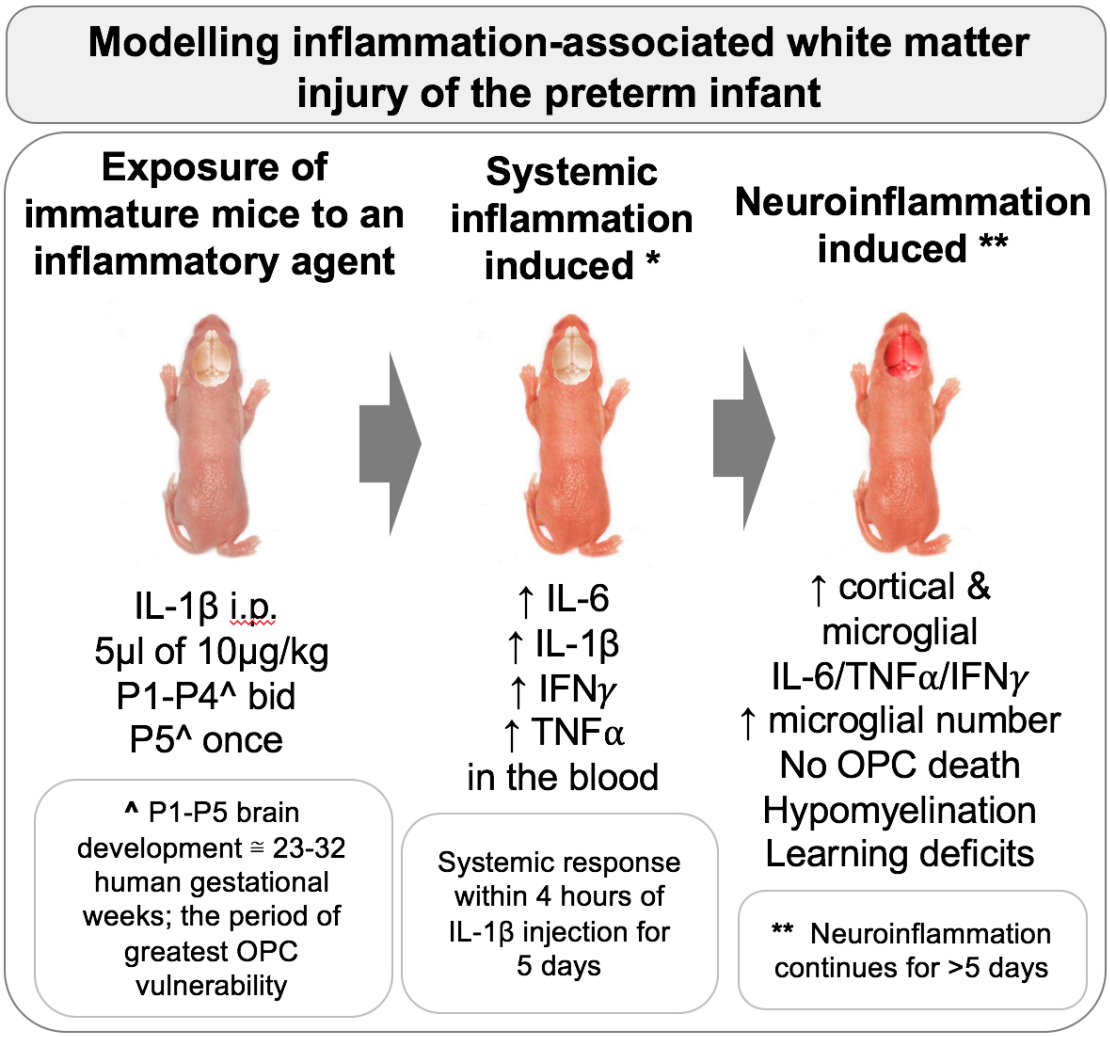

Figure 1. Outline of the model of inflammation-associated white matter injury of the preterm infant. Use of P1-P5 mice to model the preterm infant brain is supported by comparative studies of brain growth and oligodendrocyte maturation (Back et al., 2001; Dean et al., 2011; Dobbing and Sands, 1979) and reviewed in (Semple et al., 2013). Full descriptions of the model including systemic and central inflammatory response and neuropathology are available within these references (Favrais et al., 2011; Krishnan et al., 2017; Schang et al., 2014; Shiow et al., 2017; Van Steenwinckel et al., 2018). Abbreviations: IL-1β, interleukin-1β; i.p., intraperitoneal injection; P, postnatal day of life with P0 as day of birth; bid, twice daily; ≅, approximately equal to; OPC, oligodendrocyte progenitor cell.

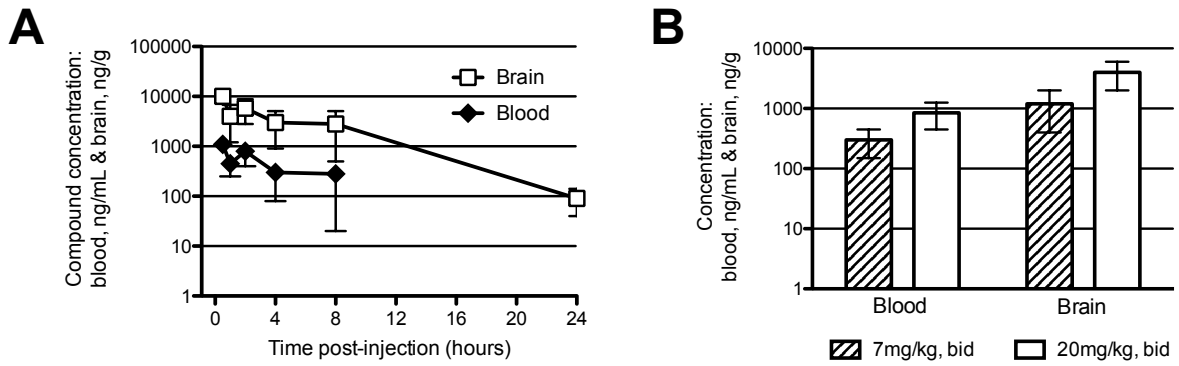

Figure 2. Pharmacokinetic data for GSK247246**. A**. GSK247246 concentrations in blood (indicated in black diamond) and brain (indicated in white square) at different time point following single i.p. injection of 20 mg/kg of GSK247246. For blood pharmacokinetic analysis, the GSK247246 concentrations of 24-hour blood samples are below the detection limit of quantification assay. **B**. GSK247246 concentrations in blood and brain 2h post last dose of 5-day dosing regimen (bid via i.p.) at low (7mg/kg) or high dose (20 mg/kg).

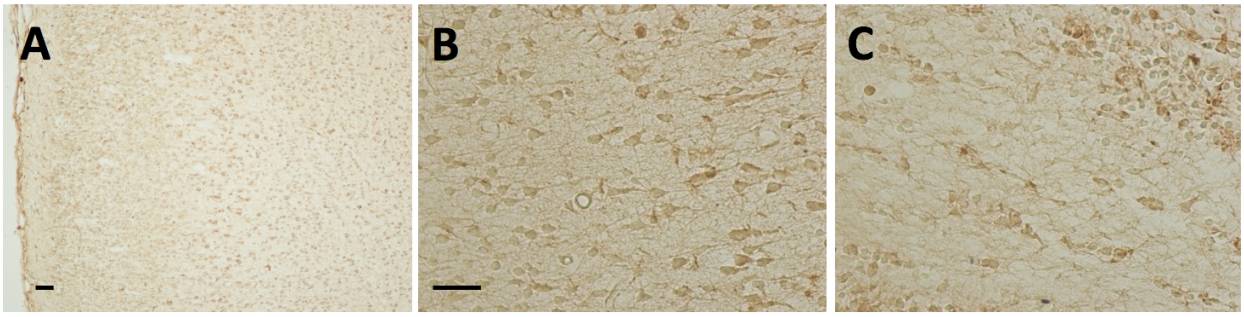

Figure 3. H3R protein expression in the developing mouse brain. H3R was observed generally at the cell membrane as expected on cells of the grey and white matter via IHC in the P5 mouse brain including in the sensorimotor cortex **A** (low magnification) & **B** (high magnification) and in the periventricular white matter **C** (high magnification). Scale bars = 100um.

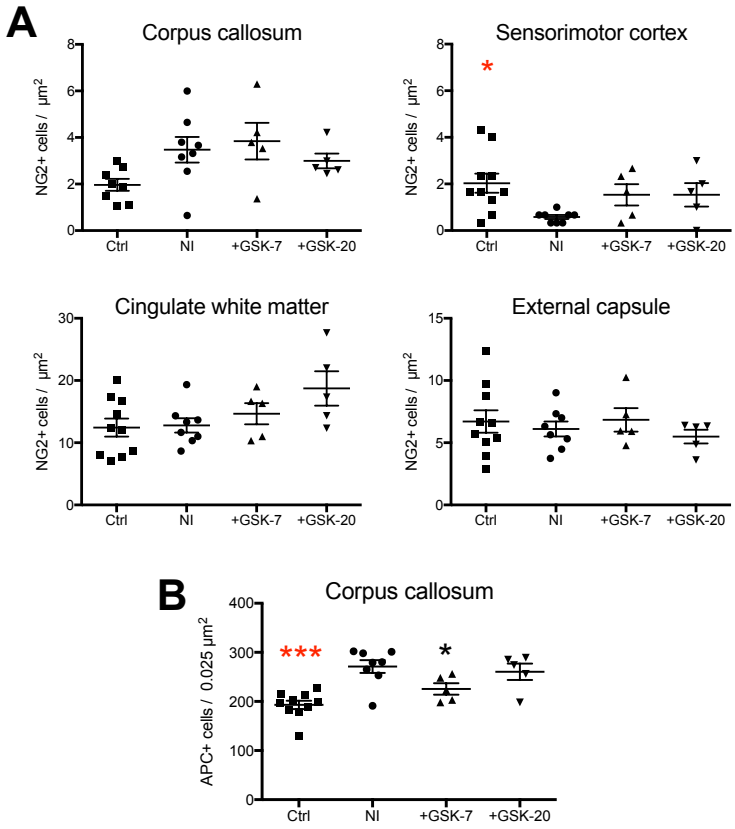

Figure 4. Effects of GSK247246 on APC and NG2 cell number in our model of PWMI. The administration of GSK247246 between P6 and P10 did not affect APC number but decreased the density of NG2 positive cells in P10 mice only in the corpus callosum with the 7 mg/kg/injection dose. **A**. Quantification of APC positive cells was assessed in mice at P10 from ≥10 litters of control (PBS treated) mice (Ctrl; n=30) or those subjected to neuroinflammation (NI; n=30), or neuroinflammation plus 7 mg/kg/injection GSK247246 (+GSK-7; n=30) and 20 mg/kg/injection GSK247246 (+GSK-20; n=30) in the corpus callosum, the sensorimotor cortex, the cingulate white matter, the external capsule. **B**. Quantification of NG2 positive cells in was assessed in mice from 5-8 litters from P10 control (PBS treated) mice (Ctrl; n=10, black bars), mice subjected to neuroinflammation (NI; n=8), or neuroinflammation plus 7 mg/kg/injection GSK247246 (+GSK-7; n=5) and 20 mg/kg/injection GSK247246 (+GSK-20; n=5) in the corpus callosum. Results are expressed as mean+/- standard deviation. Asterisks indicate statistically significant difference from NI data, *p<0.05, ***p<0.001 by Mann-Whitney test.

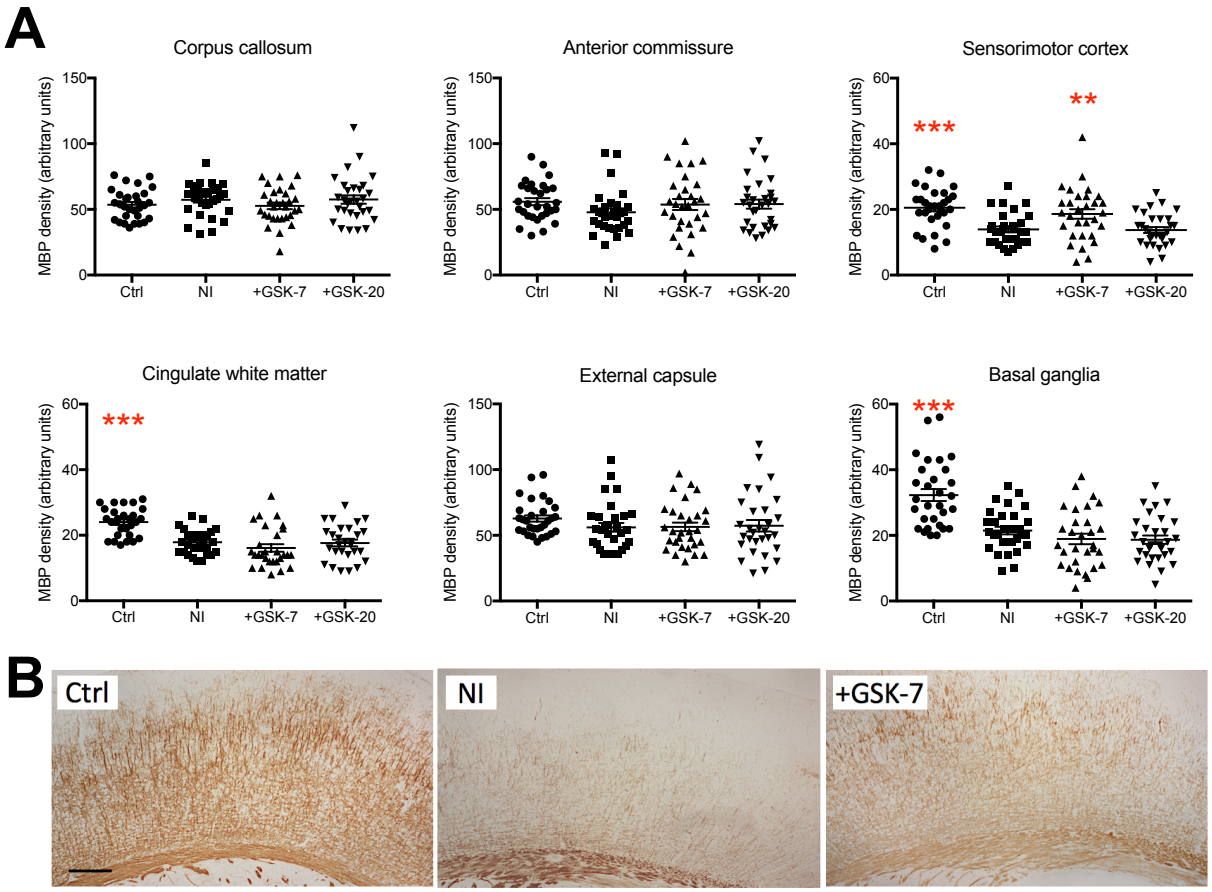

Figure 5. Effects of GSK247246 on MBP expression in our model of PWMI. The administration of GSK247246 between P6 and P10 prevented the decrease of MBP expression due to neuroinflammation in P30 mice, only in sensorimotor cortical white matter with the 7 mg/kg/injection dose. **A**. Density of MBP positive cells was assessed in mice from ≥10 litters using DAB immunostaining in P30 control PBS treated mice (Ctrl; n=30), mice subjected to neuroinflammation (NI; n=30), or neuroinflammation plus 7 mg/kg/injection GSK247246 (+GSK-7; n=30) and 20 mg/kg/injection GSK247246 (+GSK-20; n=30) within the corpus callosum, the anterior commissure, the sensorimotor cortex, the cingulate white matter, the external capsule and the basal ganglia. Results are expressed as mean+/- standard deviation. Asterisks indicate statistically significant difference from NI data, **p<0.01 and ***p<0.001 by Mann-Whitney test. **B**. Representative photomicrographs of MBP immunostaining in the sensorimotor cortex at P30 (scale bar = 100 µm).

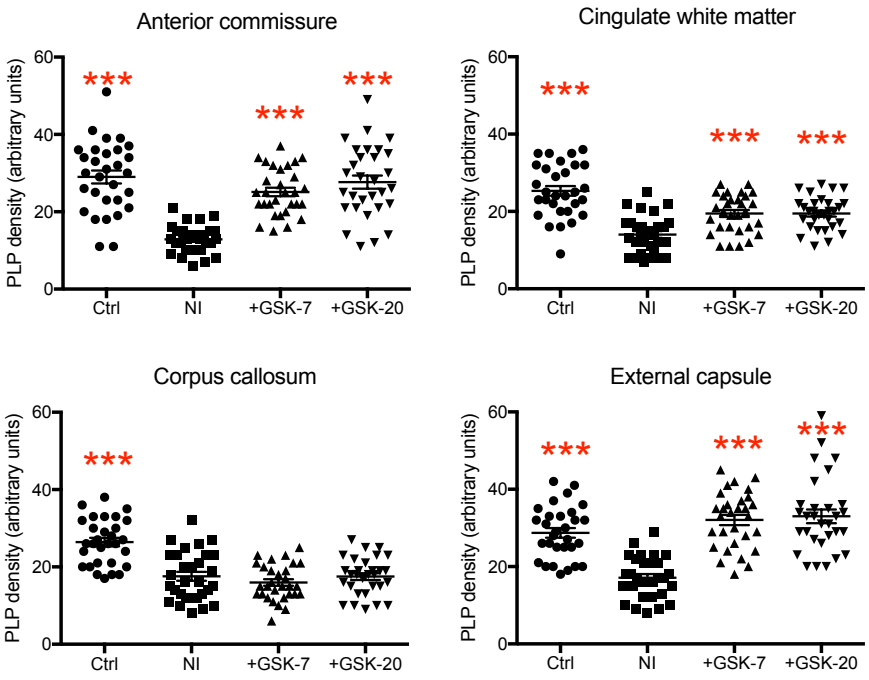

Figure 6. Effects of GSK247246 on PLP expression in our model of PWMI. The administration of GSK247246 between P6 and P10 in our model of PWMI prevented the decrease of PLP expression in P30 mice in the anterior commissure, cingulate white matter and external capsule with both doses. Density of PLP positive cells was assessed in mice from ≥10 litters using DAB immunostaining brain sections in P30 control (PBS treated) mice (Ctrl; n=30), mice subjected to neuroinflammation (NI; n=30), or neuroinflammation plus 7 mg/kg/injection GSK247246 (+GSK-7; n=30) and 20 mg/kg/injection GSK247246 (+GSK-20; n=30) within the corpus callosum, the anterior commissure, the cingulate white matter and the external capsule. Results are expressed as mean+/- standard deviation. Asterisks indicate statistically significant difference from NI data, ***p<0.001 by Mann-Whitney test.

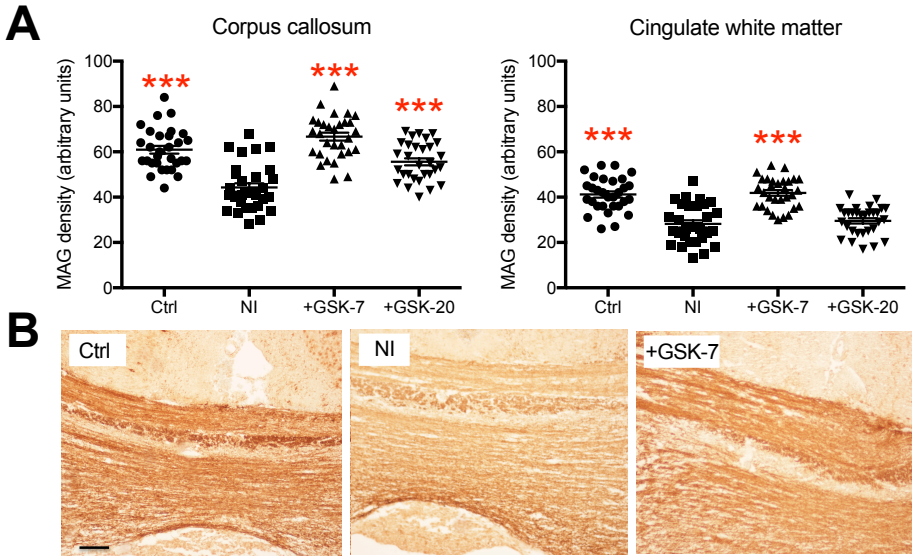

Figure 7. Effects of GSK247246 on MAG expression in our model of PWMI. The administration of 7 mg/kg/injection GSK247246 between P6 and P10 in our model of PWMI prevented the decrease of MAG in the corpus callosum and cingulate white matter. **A**. Density of MAG positive cells was assessed in mice from ≥10 litters using DAB immunostaining brain sections in P30 control (PBS treated) mice (Ctrl; n=30), mice subjected to neuroinflammation (NI; n=30), or neuroinflammation plus 7 mg/kg/injection GSK247246 (+GSK-7; n=30) and 20 mg/kg/injection GSK247246 (+GSK-20; n=30) within the corpus callosum and the cingulate white matter. Results are expressed as mean+/- standard deviation. Asterisks indicate statistically significant difference from NI data, ***p<0.001 by Mann-Whitney test. **B**. Photomicrographs of representative MAG immunostaining in the corpus callosum at P30 (scale bar = 100 µm).

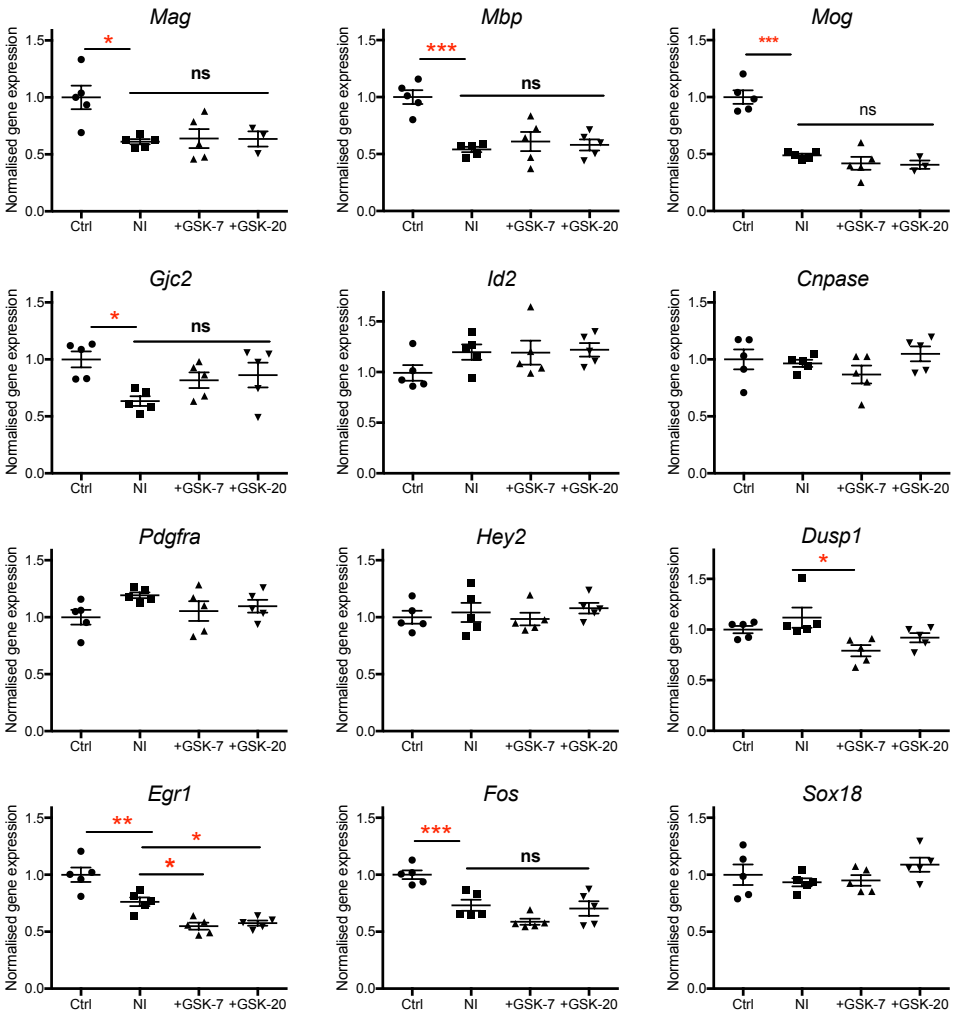

Figure 8. Effects of GSK247246 on myelin and myelin-related gene expression in our model of PWMI. Low and high doses of GSK247246 between P6 and P10 did not have significant effects on gene expression when compared to the neuroinflammation group, except for *Egr1.* Gene expression analysis of *Mag, Mbp, Mog, Gjc2, Id2, Cnpase, Pdgfra, Hey2, Dusp1, Egr1, Fos, Sox18* by qRT-PCR on frontal lobes tissue from mice from 5 litters of control mice (Ctrl; n=5), mice subjected to neuroinflammation (NI; n=5), or subjected to neuroinflammation plus 7 mg/kg/injection GSK247246 (+GSK-7; n=5) or 20 mg/kg/injection GSK247246 (+GSK-20; n=5). Results are expressed as mean+/- standard deviation. Asterisks indicate statistically significant difference from NI data, *p<0.05, **p<0.01 and ***p<0.001 by Mann-Whitney test.

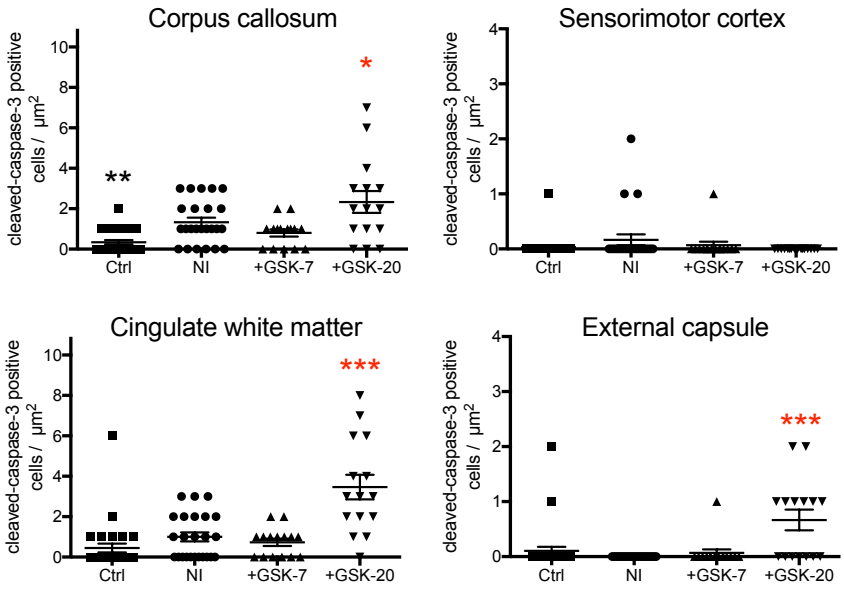

Figure 9. Effects of GSK247246 on cleaved-caspase-3 cell number in our model of PWMI. Only high dose GSK247246 significantly increased cell death in P10 mice. Quantification of cleaved caspase 3 positive cells from mice from ≥10 litters within the corpus callosum, the sensorimotor cortex, the cingulate white matter and the external capsule of P10 control mice (Ctrl; n=29), mice subjected to neuroinflammation (NI; n=24), or subjected to neuroinflammation plus 7 mg/kg/injection GSK247246 (+GSK-7; n=15) or 20 mg/kg/injection GSK247246 (+GSK-20; n=15). Results are expressed as mean+/- standard deviation. Asterisks indicate statistically significant difference from NI data, *p<0.05 and ***p<0.001 by Mann-Whitney test.

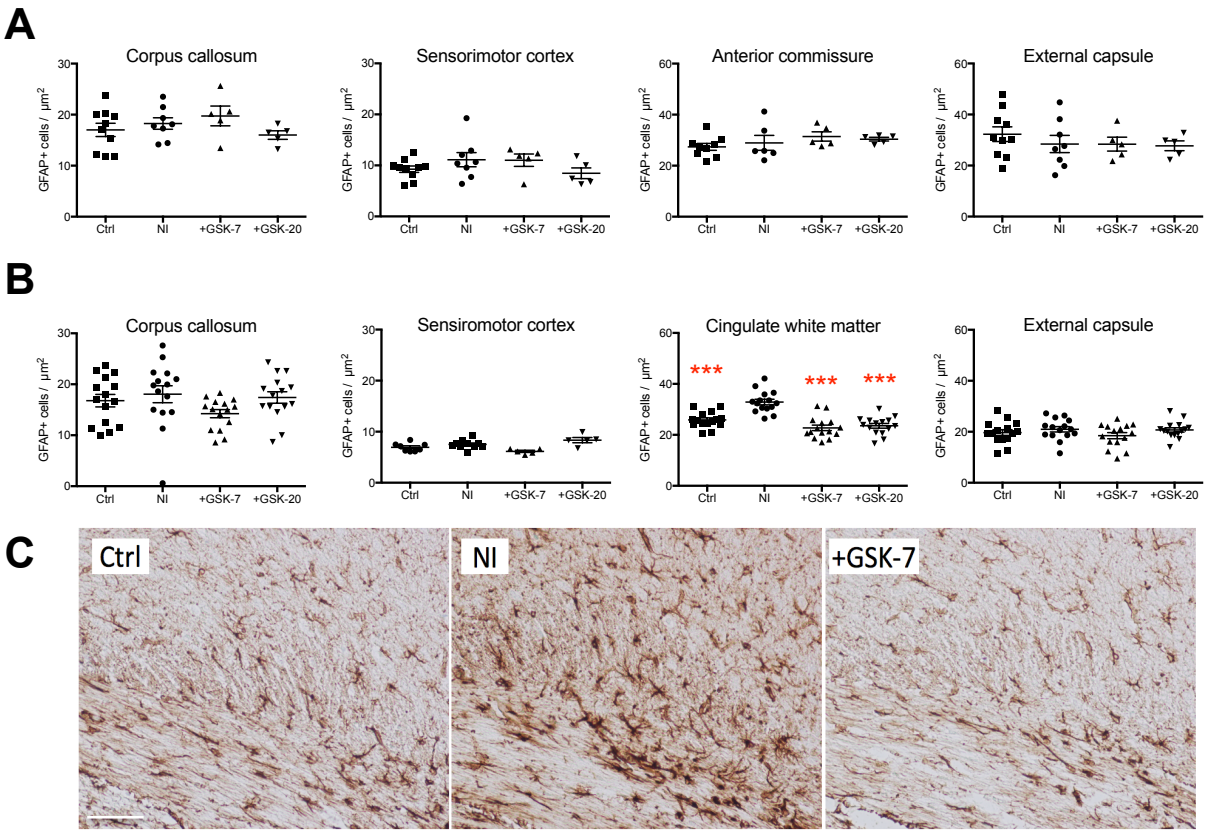

Figure 10. A. GSK247246 reduces delayed onset NI induced GFAP cell number increases. Quantification of GFAP positive cells in the corpus callosum, the sensorimotor cortex, the anterior commissure or cingulate white matter and the external capsule. **A**. Tissues were collected from 5 litters of mice at P10, from control mice (Ctrl; n=10), those subjected to neuroinflammation (NI; n=8), or subjected to neuroinflammation plus 7 mg/kg/injection GSK247246 (+GSK-7; n=5) and 20 mg/kg/injection GSK247246 (+GSK-20; n=5), or **B**. tissues were collected from ≥10 litters of mice at P30 from control mice (Ctrl; n=15), mice subjected to neuroinflammation (NI; n=15), neuroinflammation plus 7 mg/kg/injection GSK247246 (+GSK-7; n=15) or plus 20 mg/kg/injection GSK247246 (+GSK-20; n=15). Results are expressed as mean+/- standard deviation. Asterisks indicate statistically significant difference from NI data, ***p<0,001 by Mann-Whitney test. (C) Representative photomicrographs of GFAP immunostaining at the cingulate white matter level at P30 (scale bar = 100 µm).

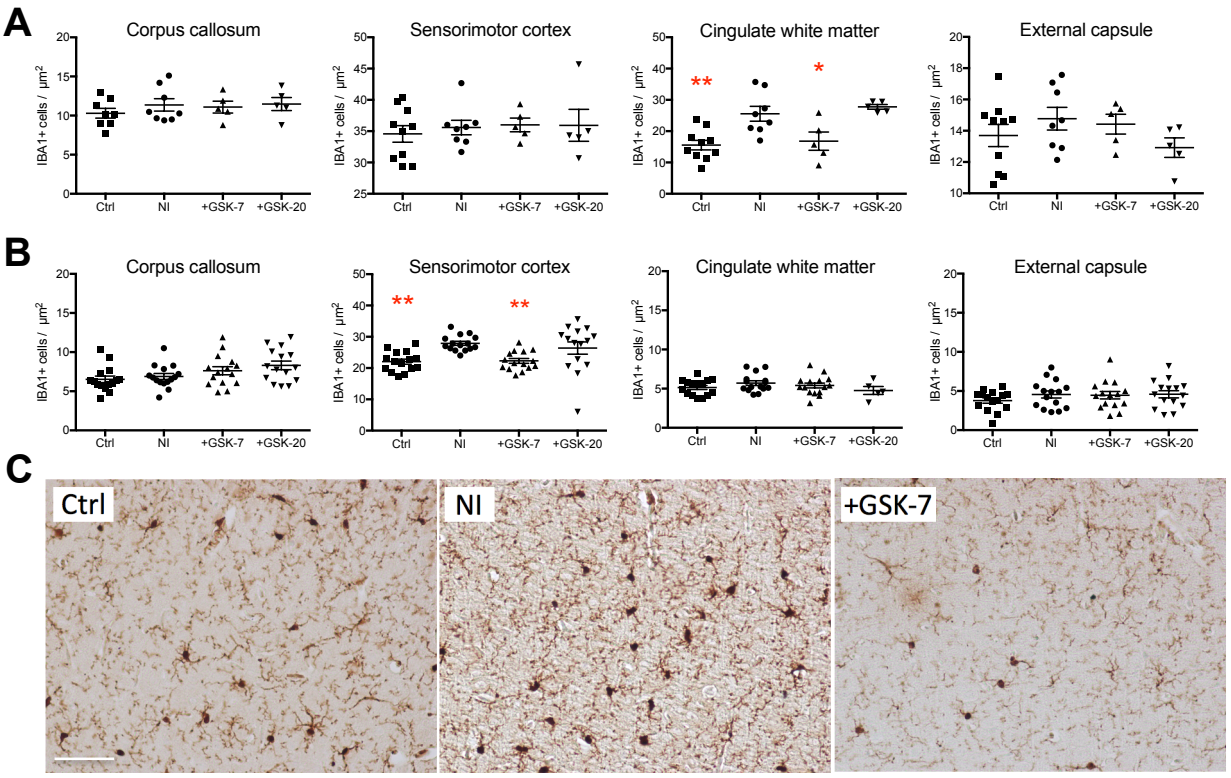

Figure 11. Increased IBA1 positive cell number in the animals subjected to neuroinflammation was reduced by GSK247246 in selected regions at P10 and P30. Quantification of IBA1 positive cells in the corpus callosum, the sensorimotor cortex, the cingulate white matter and the external capsule. **A**. Tissues were collected from 5 litters of mice at P10, from control mice (Ctrl; n=10), those subjected to neuroinflammation (NI; n=8), or subjected to neuroinflammation plus 7 mg/kg/injection GSK247246 (+GSK-7; n=5) or plus 20 mg/kg/injection GSK247246 (+GSK-20; n=5). Also **B**. from tissues from ≥10 litter at P30 mice in control mice (n=15), those subjected to neuroinflammation (n=15), neuroinflammation plus 7 mg/kg/injection GSK247246 (+GSK-7; n=15) or plus 20 mg/kg/injection GSK247246 (+GSK-20; n=15). Results are expressed as mean+/- standard deviation. Asterisks indicate statistically significant difference from NI data, *p<0.05 and **p<0.01 by Mann-Whitney test. **C**. Representative photomicrographs of IBA1 immunostaining at the sensory motor cortex level at P30 (scale bar = 100 µm).

Gene	**Sequences** (5' and 3' respectively)	**NCBI reference**	**Amplicon size**
Mag	GTCTCTACCCGGGATTGTCA	NM_010758	131
	CCCAGGTCTGAGTGGGAATA		
Mbp	CCGGACCCAAGATGAAAAC	NM-001025259	77
	CTTGGGATGGAGGTGGTGT		
Mog	AAGAGGCAGCAATGGAGTTG	NM-010814	101
	GACCTGCAGGAGGATCGTAG		
Gjc2	CCTTCCTTCCAAGGCTCTCT	NM-080454.4	146
	TGGGAGTTCTCTGGCTCTGT		
Id2	CTGGACTCGCATCCCACTAT	NM_010496	144
	CGACATAAGCTCAGAAGGGAAT		
Cnpase	AGACAGCGTGGCGACTAGACT	NM_009923	85
	GGGCTTCAGCTTCTTCAGGT		
Pdgfra	GACGTTCAAGACCAGCGAGTT	NM_011058	82
	CAGTCTGGCGTGCGTCC		
Hey2	TGAAGATGCTCCAGGCTACA	NM_013904.1	87
	CACTCTCGGAATCCAATGCT		
Dusp1	AGGACAACCACAAGGCAGAC	NM_013642.3	142
	GAGGTAAGCAAGGCAGATGG		
Egr1	GAGCGAACAACCCTATGAGC	NM_007913.5	90
	GGGATAACTCGTCTCCACCA		
Fos	ATGGGCTCTCCTGTCAACAC	NM_010234.2	77
	TGTCACCGTGGGGATAAAGT		
Sox18	CGCAGTACTGAGCAAGATGC	NM_009236.2	134
	CGAGGCCGGTACTTGTAGTT		

Supplementary table 1. Primer sequences and NCBI reference for primers for qRT-PCR.

Primary Name	Description	P5 data O4+ cells		P5 data CD11b+ cells	
		Fold Change	P Value	Fold Change	P Value
Hrh1	Mus musculus histamine receptor H1 (Hrh1), transcript variant 1, mRNA [NM_001252643]	-1.22029	0.02495	1.182	1.53E-01
Hrh1	Mus musculus histamine receptor H1 (Hrh1), transcript variant 1, mRNA [NM_001252643]	-1.03229	0.78373	-1.019	7.58E-01
Hrh1	Mus musculus histamine receptor H1 (Hrh1), transcript variant 1, mRNA [NM_001252643]	1.02724	0.56063	**-2.231**	**5.14E-05**
Hrh2	Mus musculus histamine receptor H1 (Hrh1), transcript variant 1, mRNA [NM_001252643]	1.07234	0.81063	1.446	5.26E-01
Hrh3	Mus musculus histamine receptor H3 (Hrh3), mRNA [NM_133849]	1.27853	0.01658	1.797	1.48E-01
Hrh4	Mus musculus histamine receptor H4 (Hrh4), mRNA [NM_153087]	-1.01397	0.88406	1.329	5.43E-02

Supplementary table 2. Microarray data confirmed the expression of the *H3R* mRNA in O4-positive oligodendrocytes and CD11B-positive microglia at both at P5. Data also available for P10 also showing no overt change (Krishnan et al., 2017).